A VORTEX LATTICE PROGRAM FOR STEADY STATE AERODYNAMIC ANALYSIS OF WIND TURBINE BLADE LOADS

Da Silva, C. T.[a, b], Donadon, M. V.[a], Menezes, J. C.[a], Silva, R. G. A. da[a]

[a]*Instituto Tecnológico de Aeronáutica, DCTA-ITA-IEM, Praça Marechal Eduardo Gomes, 50. Vila das Acácias. 12228-900, São José dos Campos, SP, Brasil, http://www.mec.ita.br/leica*

[b]*Universidade Tecnológica Federal do Paraná, UTFPR, Av. Sete de Setembro, 3165. Rebouças. 80230-901, Curitiba, Paraná, Brasil., http://www.damec.ct.utfpr.edu.br*

Keywords: Aerodynamics, Vortex Lattice Method, Wind turbine blade loads.

Abstract. This paper presents a revised MATLAB program for estimating the subsonic aerodynamic characteristics of an optimal design of wind turbine blades using the Vortex Lattice Method (VLM). The aerodynamic characteristics of interest are mainly pressure distribution and aerodynamic loads, but lift, rolling moment, pitching moments are also investigated. The program is developed and revised to evaluate the viability of using the VLM to carry out virtual tests in order to obtain consistent and confident data for the structural design of the wind turbine blades. Numerical results are presented, compared with classical results of the literature and discussed.

1 INTRODUCTION

Since the demand for energy, more specifically electricity, has increased dramatically over the last 100 years, it has now become important to consider the environmental impacts of energy production. Therefore, there is general agreement that to avoid energy crisis, the amount of energy needed to sustain society will have to be contained and, to the extent possible, renewable sources will have to be used. As a consequence, conservation and renewable energy technologies are going to increase in importance and reliability. Up-to-date information about their availability, efficiency, and cost is necessary for planning a secure energy future.

Within this context, this paper focuses on the development of a blade design tool for horizontal axis wind turbines with variable geometry. The design tool consists of an in-house MatLab program based on the Glauert Blade Element Theory (Burton, 2001), including tip and rotational wake losses as well as blade pitching and blade twisting effects, for the aerodynamic design. The program enables predictions of aerodynamic power, efficiency and forces acting on the wind turbine blades for a given operating condition.

One of the crucial and fundamental steps of the wind turbine blade design is the structural design. The determination of the aerodynamic loads associated with a given morphing blade configuration is essential. For this purpose, a vortex lattice based program has been also modified and presented in this paper. The program enables the prediction of lift, pitching moments, rolling moment and pressure distribution for twisted blade plan form. One sample case for a 2 MW wind turbine is present and discussed.

2 AERODYNAMICS OF WIND TURBINES AND OPTIMIZATION

Blade element theory (BET) is a mathematical process originally designed by William Froude, David W. Taylor and Stefan Drzewiecki to determine the behavior of propellers. Glauert adapted the theory to wind turbines. Blade element theory attempts to address information on rotor performance or blade design by considering the effects of blade design i.e. shape, section, twist, etc. Blade element theory models the rotor as a set of isolated two-dimensional blade elements to which we can then apply 2-dimensional aerodynamic theory individually and then perform an integration to find thrust and torque.

A model attributed to Betz (Burton, 2001), can be used to determine the power from an ideal turbine rotor. This model is based on a linear momentum theory. Assuming a decrease in wind velocity between the free stream and the rotor plane, an axial induction factor, a, can be defined as

$$a = \frac{U - U_d}{U}, \tag{1}$$

where U is the free stream wind velocity and U_d is the wind velocity at the rotor plane disk.

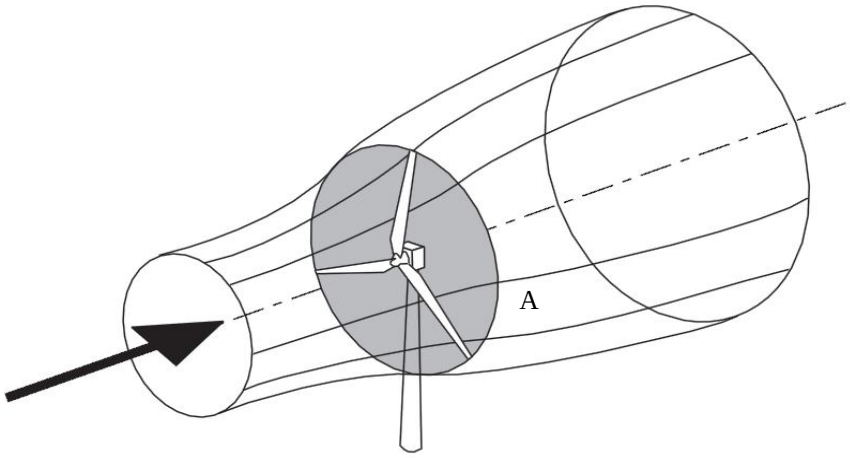

Figure 1. The energy extracting stream-tube of a wind turbine.

The governing principle of conservation of flow momentum can be applied for both axial and circumferential directions. For the axial direction, the change in flow momentum along a stream-tube starting upstream, passing through the propeller disk area and then moving off into the slipstream must be equal to the thrust produced by this element of the blade. To remove the unsteady effects due to the propeller's rotation, the stream-tube, according to Fig. 1 used is one covering the complete area, *A*, of the propeller disk swept out by the blade element and all variables are assumed to be time averaged values. The axial thrust on the rotor plane disk is given by

$$T = \frac{1}{2}\rho A U^2 \left[4a\left(1-a\right)\right], \tag{2}$$

where ρ is the air density.

The power out, *P*, is equal to the thrust times the velocity at the disk.

$$P = \frac{1}{2}\rho A U^3 4a\left(1-a\right)^2 . \tag{3}$$

Wind turbine rotor performance is usually characterized by its power coefficient, C_p, which represents the fraction of the power in the wind that is extracted by the rotor.

$$C_p = \frac{Rotor\ power}{Power\ on\ the\ wind} = \frac{P}{\frac{1}{2}\rho A U^3} . \tag{4}$$

If one considers the wake rotation, according to Fig. 2, where the angular velocity imparted to the flow stream is ω, while the angular velocity of the wind turbine rotor is Ω, then, across the flow disk, the angular velocity of the air relative to the blade increases from Ω to $\left(\omega+\Omega\right)$. One can prove that the tangential component of velocity is $\Omega r\left(1+a\right)$, according to Fig. 3. In Fig. 3 α is the angle of attack, ϕ is the angle of relative wind and β is section pitch angle. Note that the angle of the relative wind is the sum of the section pitch angle and the angle of attack.

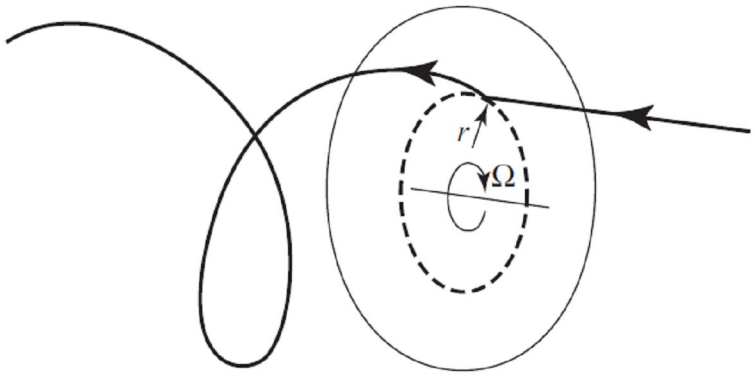

Figure 2. The trajectory of an air particle passing through the rotor disc.

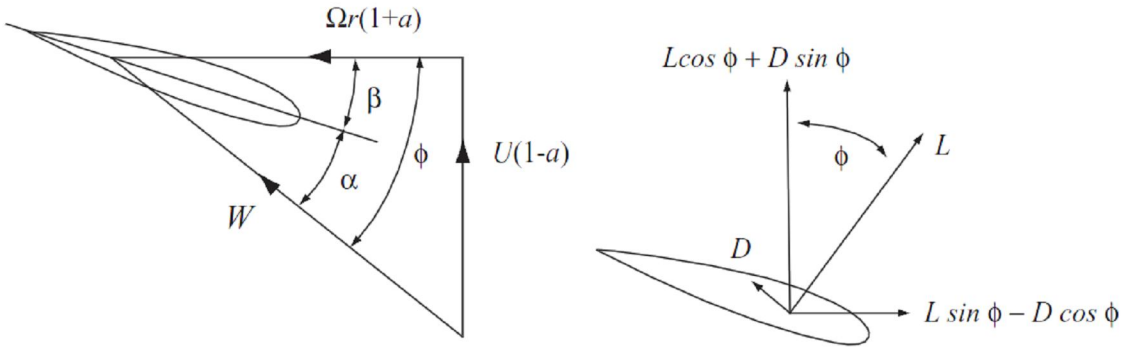

Figure 3. Blade element velocities and forces.

$$\phi = \alpha + \beta \,. \tag{5}$$

Taking into account the lift force L and the drag force D, one can define the lift and the drag coefficients as

$$C_l = \frac{\dfrac{Lift\ \ force}{unit\ lenght}}{\dfrac{Dynamic\ \ force}{unit\ lenght}} = \frac{\dfrac{L}{l}}{\dfrac{\frac{1}{2}\rho U^2 c}{l}} \tag{6}$$

and

$$C_d = \frac{\dfrac{Drag\ \ force}{unit\ lenght}}{\dfrac{Dynamic\ \ force}{unit\ lenght}} = \frac{\dfrac{D}{l}}{\dfrac{\frac{1}{2}\rho U^2 c}{l}} \,. \tag{7}$$

From Fig. 3, one can determine the following relationships:

$$W = \frac{U(1-a)}{\sin\phi}, \tag{8}$$

$$F_N = L\cos\phi + D\sin\phi \tag{9}$$

and

$$F_T = L\sin\phi - D\cos\phi, \tag{10}$$

where W is the relative wind velocity, F_N is the normal force, and F_T is the tangential force to the disk.

If the rotor has B blades, the differential normal force on the section at the distance, r, from the centre is

$$dF_N = B\frac{1}{2}\rho W^2\left(C_l\cos\phi + C_d\sin\phi\right)cdr \tag{11}$$

and the differencial torque is

$$dQ = B\frac{1}{2}\rho W^2\left(C_l\sin\phi - C_d\cos\phi\right)crdr\,. \tag{12}$$

The power coefficient can be calculated as a function of the tip speed ratio λ and the local speed ratio λ_r (Gash and Twele, 2002) by

$$C_p = \frac{8}{\lambda^2}\int_{\lambda_h}^{\lambda}\sin^2\phi\left(\cos\phi - \lambda_r\sin\phi\right)\left(\sin\phi + \lambda_r\cos\phi\right)\left[1 - \frac{C_d}{C_l}\cot\phi\right]\lambda_r^{\,2}d\lambda_r, \tag{13}$$

where

$$\lambda = \frac{\Omega R}{U} \tag{14}$$

and

$$\lambda_r = \lambda\frac{r}{R}, \tag{15}$$

One can perform the optimization of the blade shape for an ideal rotor by taking the partial derivative of C_p which is a function of ϕ, and setting it equal to zero, to reveal that

$$\phi = \frac{2}{3}\tan^{-1}\left(\frac{1}{\lambda_r}\right) \tag{16}$$

and

$$c = \frac{8\pi r}{BC_l}\left(1 - \cos\phi\right). \tag{17}$$

Applying the Blade Element Theory (Donadon et al., 2008), the total wind turbine thrust and torque is obtained by summing the results of all the radial blade elements along the radial direction.

$$\begin{aligned} T &= \sum_{i=1}^{N} \Delta T \\ Q &= \sum_{i=1}^{N} \Delta Q \end{aligned}, \tag{18}$$

where N is the number of blade elements along the radial direction.

3 VORTEX LATTICE METHOD (VLM)

In order to determinate the aerodynamic load, a computational program was developed based on the Vortex Lattice Method (VLM) (Donadon and Iannucci, 2006). This section presents a short review on the VLM method and the fundamental equations used in the numerical implementation.

The VLM method is the simplest of the methods to solve incompressible flows around wings of finite span (Bertin, 1989). The method represents the wing as a planar surface on which grids of horseshoe vortex are superimposed. The computation of the velocities induced by each horseshoe vortex at each specified control point is based on the Biot-Savart law (Bertin, 1989). A summation is performed for all control points on the wing to produce a set of linear system of equations for the horseshoe vortex strengths that satisfy the boundary conditions of no flow through the wing. The control points of each element (or lattice) are located at three-fourth of the element's chord and the vortex strengths are related to the wing circulation and the pressure difference between the upper and lower surface of the wing. The pressure differentials are then integrated to yield the total forces and moments. In the approach used here to solve the governing equations, the continuous distribution of bound vorticity over the wing surface is approximated by a finite number of discrete horseshoe vortices, as shown in Fig. 4. The individual horseshoe vortices are placed in rectangular (or trapezoidal) panels also called finite elements or lattices. This procedure for obtaining a numerical solution for the flow is termed Vortex Lattice Method. The bound vortex coincides with quarter-chord line of the element and is therefore, aligned with the local sweepback angle. In a rigorous theoretical analysis, the vortex lattice panels are located on the mean chamber of the wing and, when the trailing vortices leave the wing, they follow a curved path. However, for many engineering applications, suitable accuracy can be obtained linearized theory in which straight line vortices extend downstream to infinity.

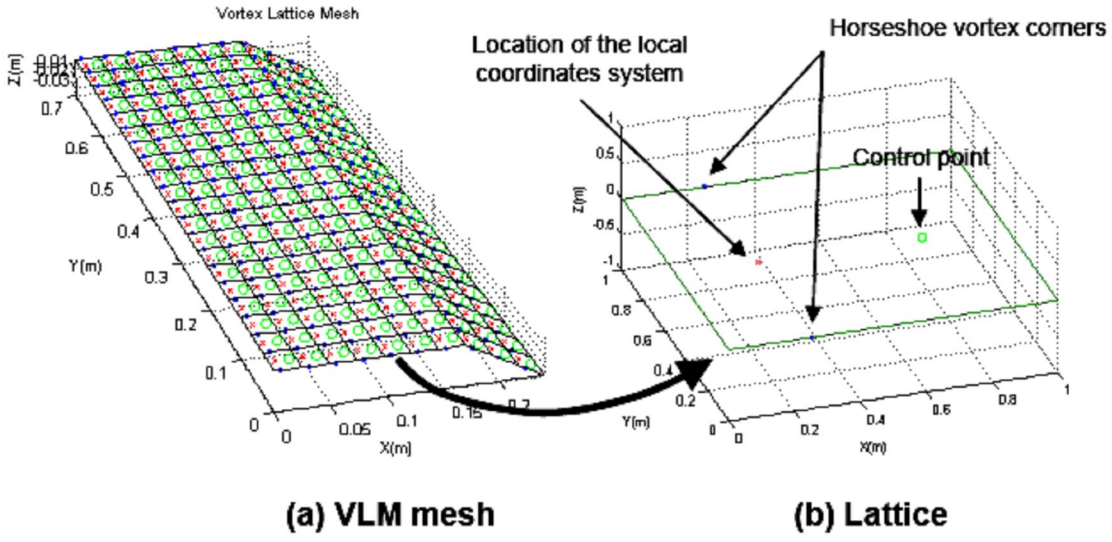

Figure 4. Vortex Lattice discretization.

The easy implementation, high speed running and consistent result are the most important reasons to adopt this method to calculate the aerodynamic load. This procedure will make possible an optimization routine that is the final objective of the entire project this work is inside on.

3.1 Velocity induced by a general horseshoe vortex

Let's assume a typical three dimensional horseshoe vortex composed by a bound vortex segment and two trailing vortex segments as shown in Fig. 5.

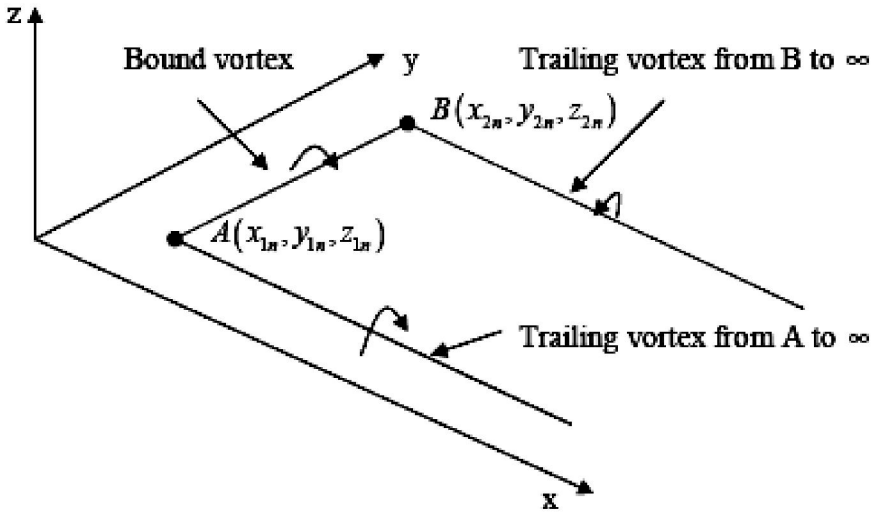

Figure 5. Typical horseshoe vortex.

The computation of the velocity induced at some point $C(x,y,z)$ by a vortex segment AB for instance (See Fig.5) is based on the Biot and Savart law as follows (Bertin, 1989),

$$\vec{V}_{AB} = \frac{\Gamma_n \cdot \vec{r}_1 \times \vec{r}_2}{4\pi \left| \vec{r}_1 \times \vec{r}_2 \right|^2} \left[\vec{r}_0 \left(\frac{\vec{r}_1}{r_1} - \frac{\vec{r}_2}{r_2} \right) \right]. \tag{19}$$

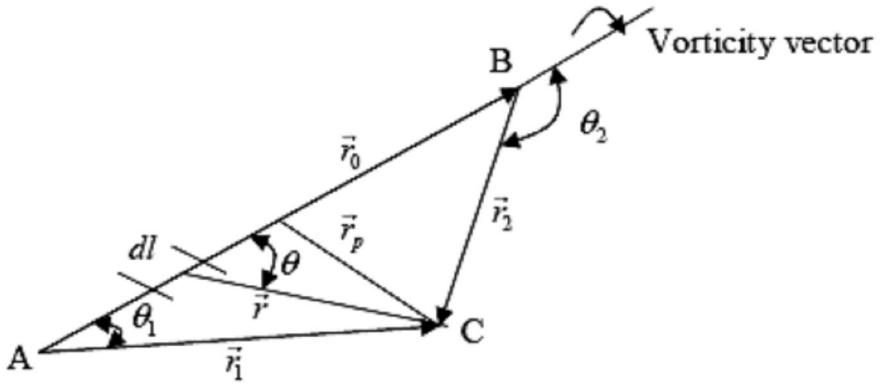

Figure 6. Vortex segment AB.

To calculate the velocity induced by the filament that extends from A to ∞, let us first calculate the velocity induced by the collinear, finite-length filament that extends from A to D according to Fig. 7.

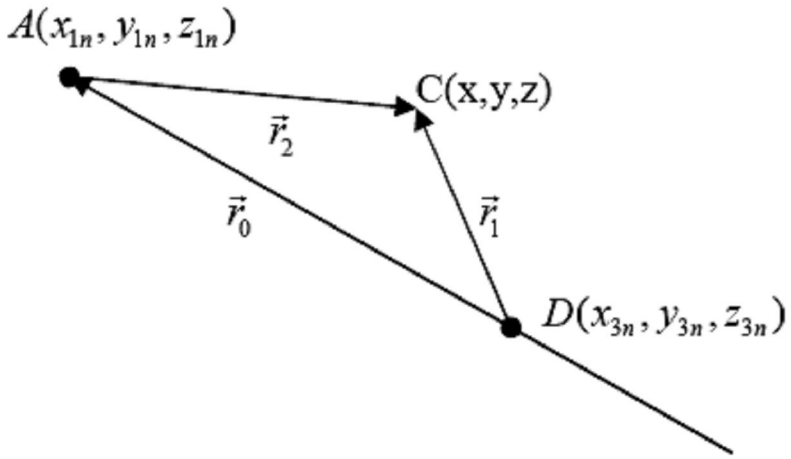

Figure 7. Vortex segment A∞.

Applying again Biot and Savart law one can show that the velocity induced by the filament that extends from A to ∞ is given by,

$$\vec{V}_{A\infty} = \frac{\Gamma_n}{4\pi} \left\{ \frac{(z - z_{1n})j + (y - y_{1n})k}{(z - z_{1n})^2 + (y_{1n} - y)^2} \right\} \left[1 + \frac{x - x_{1n}}{\sqrt{(x - x_{1n})^2 + (y - y_{1n})^2 + (z - z_{1n})^2}} \right]. \tag{20}$$

Similarly, the velocity induced by the vortex filament that extends from B to ∞ is written as,

$$\vec{V}_{B\infty} = \frac{\Gamma_n}{4\pi}\left\{\frac{(z-z_{2n})j+(y-y_{2n})k}{(z-z_{2n})^2+(y_{2n}-y)^2}\right\}\left[1+\frac{x-x_{2n}}{\sqrt{(x-x_{2n})^2+(y-y_{2n})^2+(z-z_{2n})^2}}\right]. \quad (21)$$

The total velocity induced at some point (x,y,z) by the horseshoe vortex representing one of the surface elements with trailing vortices parallel to x-axis is

$$\vec{V} = \vec{V}_{AB} + \vec{V}_{A\infty} + \vec{V}_{B\infty}. \quad (22)$$

where the total velocity is the sum of the contributions from the three vortex segments shown in Fig.4. Assuming the point $C(x,y,z)$ to be the control point of the *mth* panel, with coordinates (x_m, y_m, z_m) located at midspan of the element and three-fourth of the elemental chord, we can express the velocity induced at the *mth* control point by the vortex representing the *nth* panel as,

$$\vec{V}_{m,n} = \vec{C}_{m,n}\Gamma_n = \left(C^u_{m,n}i + C^v_{m,n}j + C^w_{m,n}k\right)\Gamma_n. \quad (23)$$

where the influence coefficient *C* depends on the geometry of the *nth* panel and its distance from the control point of the *mth* panel. Since the governing equation is linear, the velocities induced by the *2N* vortices are added together to obtain an expression for the total induced velocity at the *mth* control point:

$$\vec{V}_m = \vec{C}_{m,n}\Gamma_n = \sum_{n-1}^{2N}\left(C^u_{m,n}i + C^v_{m,n}j + C^w_{m,n}k\right)\Gamma_n. \quad (24)$$

3.2 Computation of the vortex strengths

To compute the strengths of the vortices Γ_n which represent the lifting flow field of the wing, we use the boundary condition that the surface is a streamline. That is, the resultant flow is tangent to the wing at each and every control point. If the flow is tangent to the wing, the component of the induced velocity normal to the wing at the control point balances the normal component of the free-stream velocity. By doing that we can obtain the vortex strengths solving the following linear system of equations (Bertin, 1989),

$$\{\Gamma_n\} = \left[\overline{C}^w_{m,n} - \overline{C}^v_{m,n}\tan(\phi)\right]^{-1} 4\pi U_\infty \{\alpha_m\}. \quad (25)$$

where U_∞, ϕ and α_m are the flow velocity, wing dihedral angle and elemental local angle of attack at the *mth* control point. The derivation of the elemental local angle of attack is based on Fig.8 and is given by

$$\alpha_m = a\cos\left(\frac{\vec{U}\cdot(\vec{p}_1\times\vec{p}_2)}{|\vec{U}||\vec{p}_1\times\vec{p}_2|}\right) - \frac{\pi}{2}. \quad (26)$$

with $\vec{U} = U_\infty\cos(\alpha_i)i + U_\infty\sin(\alpha_i)j$ where α_i is the angle of attack associated with the incident flow in the plane xz.

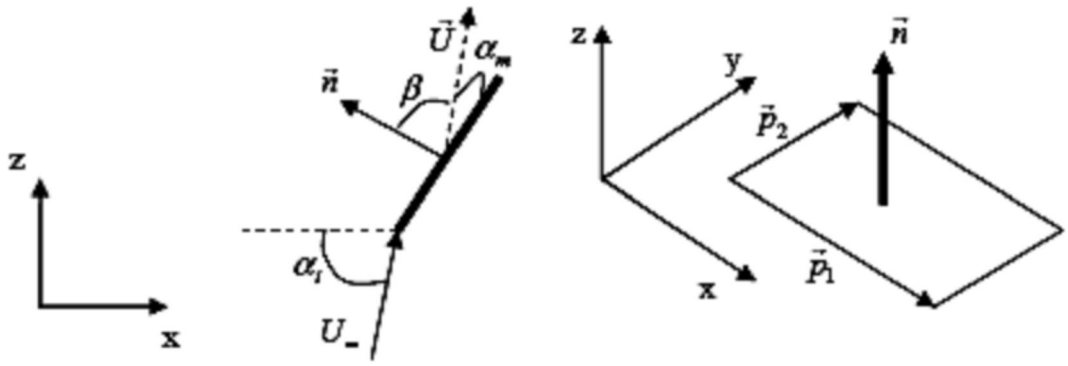

Figure 8. Elemental angle of attack.

3.3 Lift computation

Having determined the strength of each of the vortices, the lift of the wing may be calculated. The expression to compute the local lift acting on the *nth* panel of a wing with no dihedral is given by (Bertin, 1989),

$$\Delta l_n = l = \rho_\infty U_\infty \Gamma_n . \tag{27}$$

which is also the lift per unit of span. The total lift of a wing subjected to a symmetric flow is

$$L = 2\rho_\infty U_\infty \sum_{n=1}^{N} \Gamma_n . \tag{28}$$

where N is the number of panels of half-wing, Δl_n is the elemental span length and ρ_∞ is the air density.

3.4 Lift coefficient calculation

The expression for the lift coefficient is given by

$$C_L = \frac{L}{q_\infty S_{ref}} = \frac{4}{S_{ref}} \sum_{n=1}^{N} \frac{\Gamma_n}{U_\infty} \Delta y_n . \tag{29}$$

with $q_\infty = \frac{1}{2}\rho_\infty U_\infty^2$ and $S_{ref} = 0.5 s_l (c_r - c_t)$, where s_l , c_r and c_t are the wing's semi span length, wing's root chord and wing's tip chord, respectively.

3.5 Pitching moments calculation

The formulation presented here enables the computation of pitching moments about two reference lines, named leading line and flapping line (if the wing is flapped) or twisting line (if the wing is twisted). The position of these lines within the mesh is specified by the user and they are shown in Fig.8. The calculation of the pitching moments about the flapping or twisting lines is a fundamental step in the design process because it allows optimization studies to be carried out for different morphing wing configurations. It also helps in the choice of candidate materials for the deformable parts of the morphing wing enabling the computation power

required to achieve a given morphing level. For both flapped and twisted wings the pitching moment about the leading line is given by

$$M_y = 2\rho_\infty U_\infty \sum_{n=1}^{N} \Gamma_n \Delta y_n x_n^{\ b}. \tag{30}$$

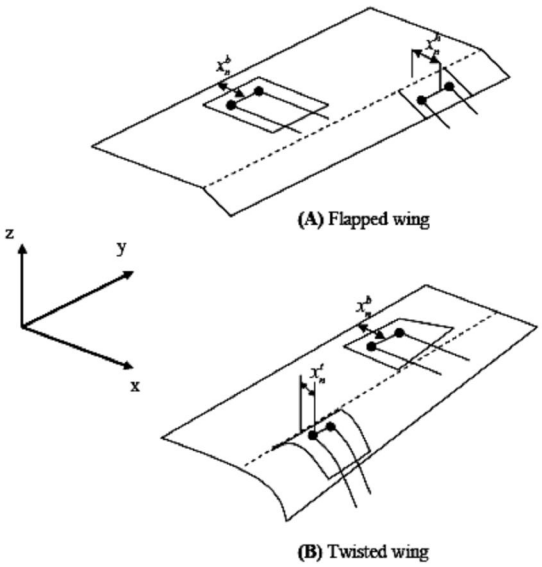

Figure 9. Reference points for pitching moment calculation.

where $x_n^{\ b}$ is the distance between the bound vortex filament of each element and the leading line reference, as shown in Fig.9. For flapped wing the pitching moment about the hinge line (or flapping line) is

$$M_y^{\ h} = 2\rho_\infty U_\infty \sum_{n=1}^{N} \Gamma_n \Delta y_n x_n^{\ h}. \tag{31}$$

where only the lift contributions of the elements ahead of hinge line is considered. In a similar way the pitching moment about the twisting line is given by

$$M_y^{\ t} = 2\rho_\infty U_\infty \sum_{n=1}^{N} \Gamma_n \Delta y_n x_n^{\ t}. \tag{32}$$

where again only the lift contributions of the elements ahead of the twisting line are considered in the calculation.

3.6 Rolling moment calculation

The rolling moment about X-axis of a semi-wing is computed by summing the lift contributions of each strip of elements along the semi-span direction multiplied by the distance of the elemental control points from the root chord as shown in Fig.10,

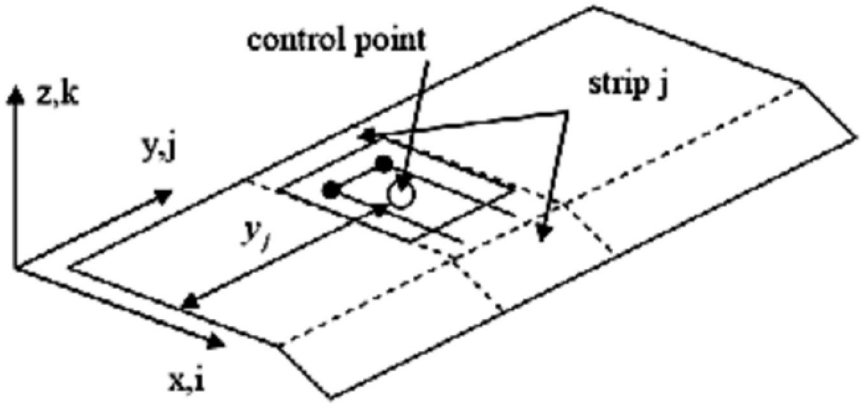

Figure 10. Reference points for pitching moment calculation.

$$M_x = \sum_{j=1}^{j_{max}} \left(\sum_{i=1}^{j_{max}} \rho_\infty U_\infty \Gamma_i \right) y_j . \tag{33}$$

where i_{max} and j_{max} are the maximum number of elements in the chordwise and spanwise directions, respectively.

3.7 Moment coefficients calculation

The expressions for the pitching moment coefficients about the leading line, flapping line and twisting line are respectively,

$$C_m = \frac{M_y}{q_\infty S_{ref} c_{ref}} . \tag{34}$$

$$C_m^h = \frac{M_y^h}{q_\infty S_{ref} c_{ref}} . \tag{35}$$

$$C_m^t = \frac{M_y^t}{q_\infty S_{ref} c_{ref}} . \tag{36}$$

with $c_{ref} = 0.5(c_{root} + c_{tip})$, where c_{root} and c_{tip} are the root chord and tip chord dimensions, respectively.

3.8 Incremental pressure coefficient calculation

The incremental pressure coefficient for the $n-th$ element is given by (Margason, 1971),

$$\Delta c_{p,n} = \frac{2\Gamma_n}{c_n U_\infty} . \tag{37}$$

where c_n is the elemental chord.

3.9 Aerodynamic energy calculation

The term aerodynamic energy defined here refers to the total energy generated by the total moments acting on the deformable parts of the wing only. For a flapped wing the expression for aerodynamic energy is given by

$$W_h = \int_0^{\theta_f} M_y^h(\theta) d\theta \,. \tag{38}$$

where θ is the flap deflection. In a similar way the aerodynamic energy for twisted wings is written as

$$W_t = \int_0^{\theta_f} M_y^t(\phi) d\phi \,. \tag{39}$$

where ϕ is the maximum twisting angle at the tip of the wing.

4 SOLUTION PROCEDURE FOR BLADE ELEMENT THEORY

The analysis described here assumes that all fluid particles undergo the same loss of momentum, i.e., there are a sufficient number of blades on the rotor for every fluid particle passing through the rotor disc to interact with a blade. With a small number of blades some fluid particles will interact with them but most will pass between the blades and, clearly, the loss of momentum by a particle will depend on its proximity to a blade as the particle passes through the rotor disc. If the axial flow induction factor a is large at the blade position then the inflow angle will be small and the lift force will be almost normal to the rotor plane. The component of the lift force in the tangential direction will be small and so will be its contribution to the torque. A reduced torque means reduced power and this reduction is known as tip loss because the effect occurs only at the outermost parts of the blades. In agreement with Burton (2001) this tip loss can be described with Prandtl's approximation by

$$f_T(\mu) = \frac{2}{\pi}\cos^{-1} e^{\left(-\frac{\frac{B}{2}(1-\mu)}{\mu}\right)\sqrt{1+\frac{(\lambda\mu)^2}{(1-a)^2}}} \,. \tag{40}$$

where $\mu = \dfrac{r}{R}$.

At the root of a blade the circulation must fall to zero as it does at the blade tip and so it can be presumed that a similar process occurs. The blade root will be at some distance from the rotor axis and the airflow through the disc inside the blade root radius will be at the free-stream velocity. It is usual, therefore, to apply the Prandtl tip-loss function at the blade root as well as at the tip.

$$f_R(\mu) = \frac{2}{\pi}\cos^{-1} e^{\left(-\frac{B}{2}\left(1-\frac{\mu_R}{\mu}\right)\right)\sqrt{1+\frac{(\lambda\mu)^2}{(1-a)^2}}} \,. \tag{41}$$

where μ_R refers the position of the hub.

So, the tip/root loss factor is written as

$$f(\mu) = f_T(\mu)\, f_R(\mu). \tag{42}$$

The tip/root loss factor leads to the new value of the induction factor.

$$a = \frac{1}{3} + \frac{1}{3} f - \frac{1}{3}\sqrt{1 - f + f^2}\,. \tag{43}$$

Once this induction factor is know, its derivative also is obtained.

$$a' = \frac{1}{(\lambda\mu)^2} a\left(1 - \frac{a}{f}\right). \tag{44}$$

The derivative of Eq. 13 with respect to μ now can be written. It represents the span-wise variation of power extraction in the presence of losses.

$$R\frac{dC_p}{dr} = 8(1-a)a'\lambda^2\mu^3. \tag{45}$$

The new inflow angle can be determined by

$$\phi = \tan^{-1}\frac{1 - \dfrac{a}{f}}{\lambda\mu\left(1 + a\dfrac{1 - \dfrac{a}{f}}{f(\lambda\mu)^2}\right)}. \tag{46}$$

The power coefficient can be found now. Considering the Blade Element Theory already nominated and using equation 46, the C_p is obtained by a summation of all blade elements. Once C_p is already estimated, the diameter of the rotor can be found.

5 NUMERICAL SIMULATION

The theory presented was used to predict the aerodynamic performance of a 2 MW wind turbine.

The wind turbine has three blades equally spaced along the circumferential direction. For the present work, the aerodynamic characteristic curves in terms of lift coefficient versus angle of attack and drag coefficient versus angle of attack of a NACA 4412 airfoil was taken into account. The adopted criterion for choosing the best airfoil for the wind turbine blade is based on how much aerodynamic power the airfoil can effectively generate and transfer to the wind turbine shaft for a given operating condition. This quantity is measured by the power coefficient C_p which is defined by the ratio between aerodynamic power and wind power, (Gash and Twele, 2002). The turbine's aerodynamic performance was evaluated for each one of the three airfoils described previously using an in-house MatLab program based on the *Glauert Blade Element Theory* cited in section 2 (Menezes and Donadon, 2009). For the studied case here the same airfoil is used in all sections of the blade along the radius direction.

Table 1 presents values of the input data U (free flow velocity) and N (number of blade elements), adopted for the numerical simulation. The same table also presents final values for R, T and Q. For the simulated case, the air properties were considered for sea level at 20^0C.

It is very important to explain here that the value of C_p found (around 0.54) refers only to the aerodynamic performance of the blade considering the Blade Element Theory. It is very high when compared with values encountered on the literature. For that reason it is not cited here.

U	12.5 m/s
N	90
R	35.4
T	1.83×10^4 N
Q	4.95×10^4 N.m

Table 1: Initial data and final results for a 2 Mw wind turbine blade.

Figure 11 shows the behavior of the blade chord along the blade radius direction. Figure 12 presents the variation of twist along the radius direction. The chord *c* is normalized according to the value of *R*.

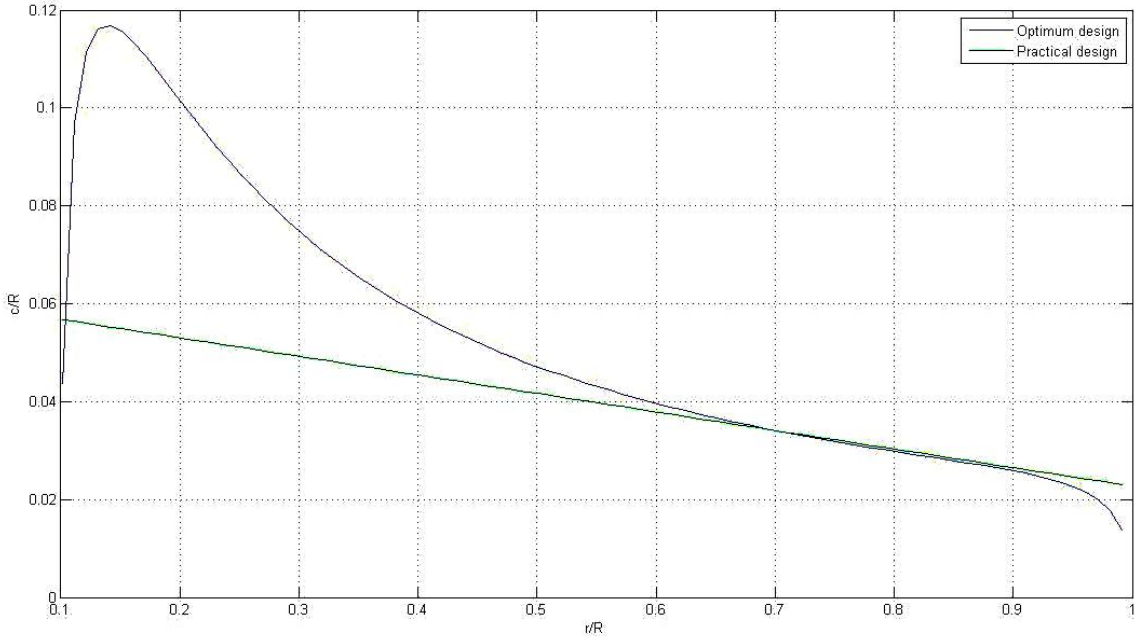

Figure 11. Blade chord along the blade radius direction.

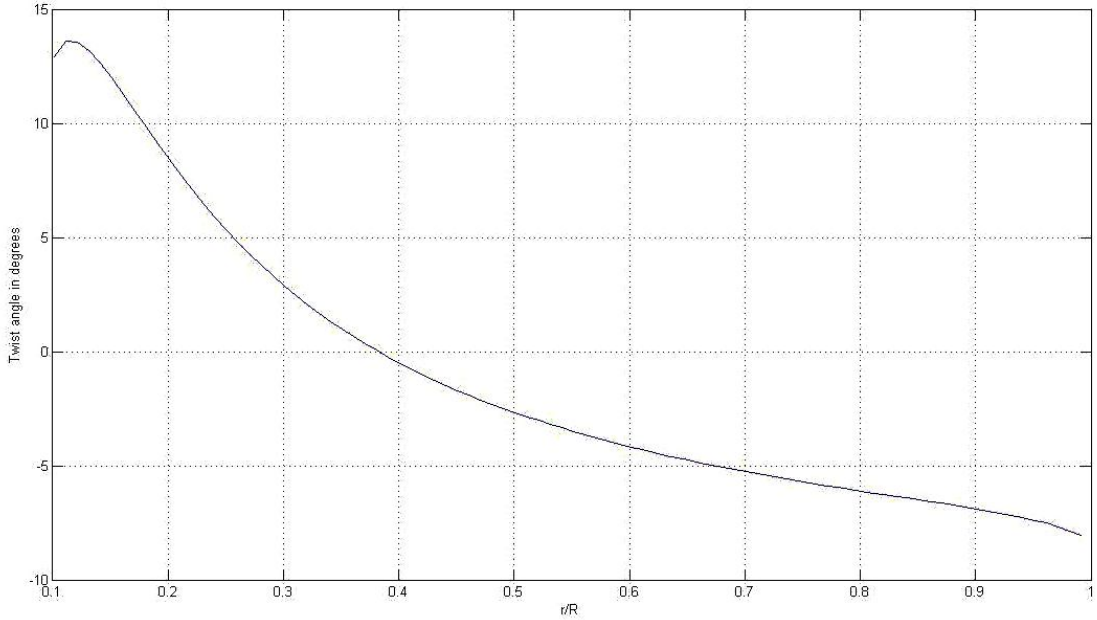

Figure 12. Variation of twist angle along the radius direction.

This data are used to construct the geometric model for the VLM.

But now it is very useful to say a commentary. At this stage of the work the most important is to ensure the technique produces consistent results. Some simplification hypothesis is used in order to facilitate the acquisition of these results on a simple manner. One the consistency of the results are achieved the simplifications will be removed and better accuracy will be reached.

For that simplification, the practical design is used and the variation of the local angle of attack for each blade section is linearized by its initial and final values.

The figure 13 shows the Vortex Lattice mesh produced using the practical design above and the linearized twist distribution. For the blade span of 35.41 meters, the root chord is of 1.61 meters and tip chord is of 0.66 meters. The twist angle is also simplified using a linear distribution of the twist along the blade span. The total twist is of 21 degrees.

The Vortex Lattice mesh has 36 elements spanwise and 16 elements chordwise is obtained. It is shown on figure 13. It is possible to see the nodes and the control points all over de vortex lattice mesh.

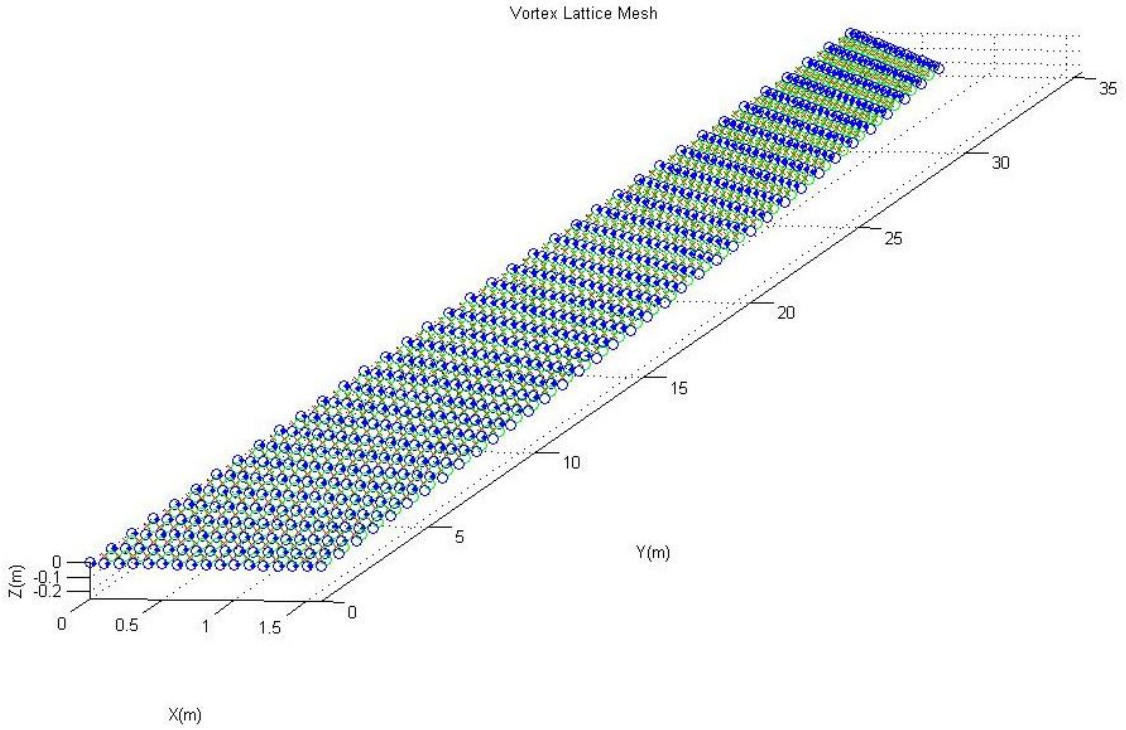

Figure 13. Vortex Lattice mesh.

The principal result obtained at this point of the work is the pressure distribution over the blade span. With the pressure distribution, or the lift distribution, is possible to obtain the loads all over the blade structure. These results are shown on figures 14 and 15.

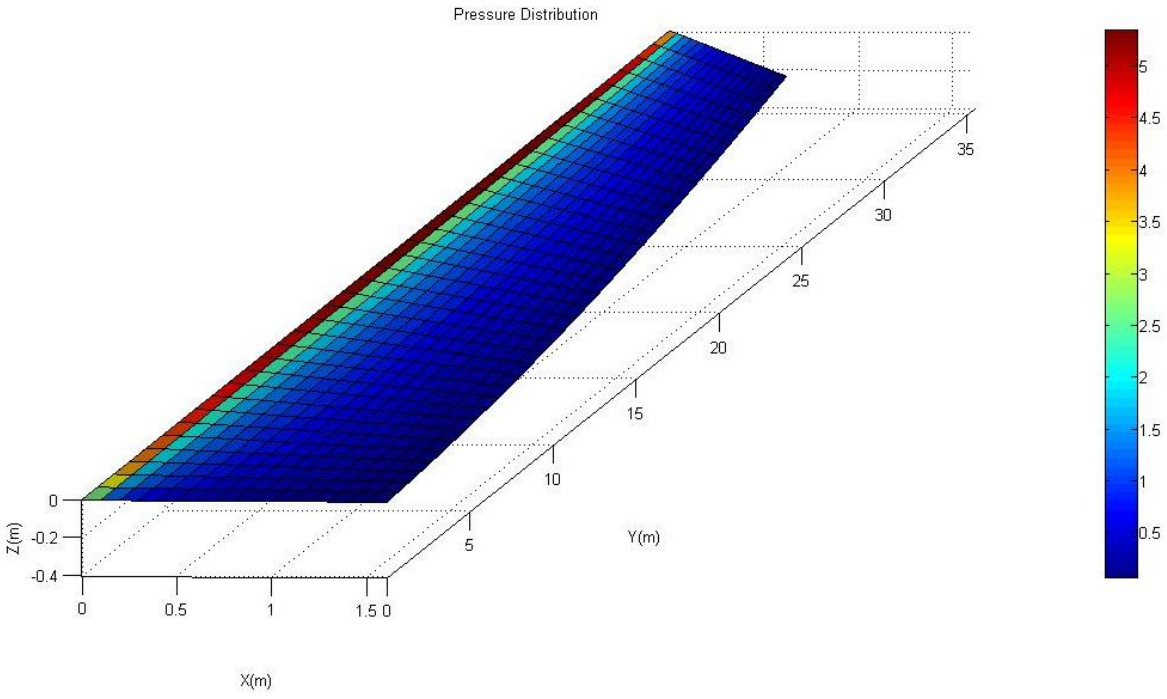

Figure 14. Pressure distribution fring.

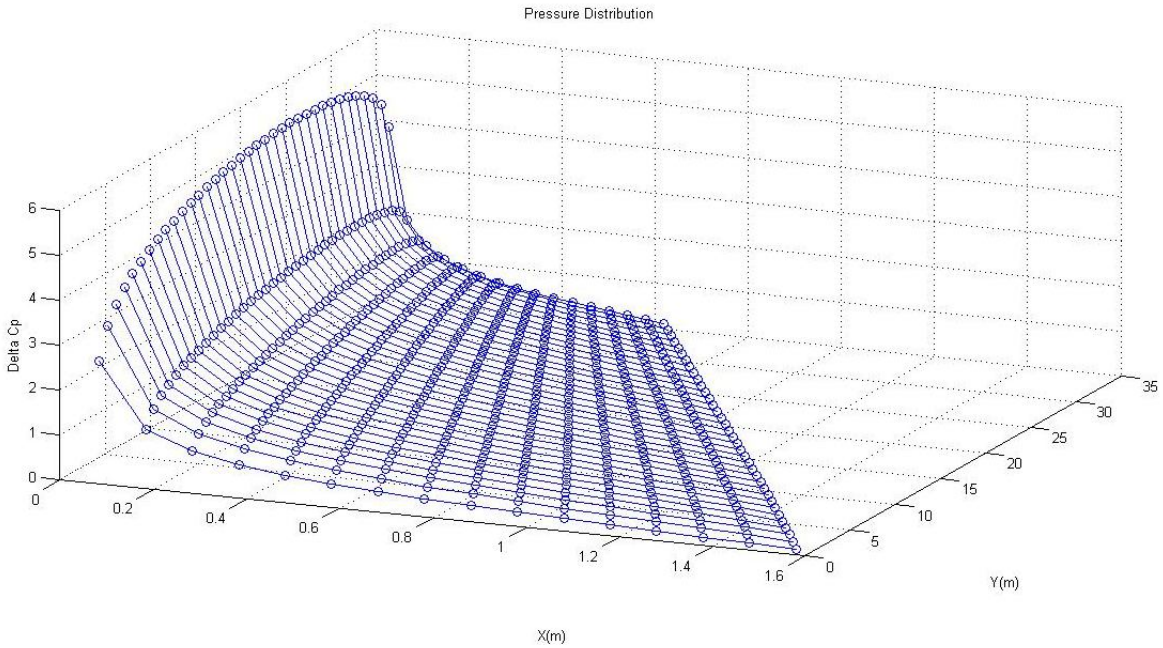

Figure 15. Pressure distribution graph.

The total lift coefficient of the blade is $C_L = 3.525$ and the total torsion coefficient due the the twist is $C_M = 0.985$.

6 CONCLUSIONS

An aerodynamic model for wind turbines with variable geometry was presented and discussed in this work. Details about the numerical implementation were also presented and discussed. The proposed formulation is based on the Glauert Blade Element Theory which accounts for tip and rotational wake losses described with Prandtl's approximation, which enables the prediction of torque, thrust and power coefficient for wind turbines with different airfoils geometries and subjected to a wide range of operating conditions. A study case in terms of aerodynamic performance was presented for a 2.0 MW wind turbine, in which a nominal velocity of 12.5 m/s was considered. The numerical predictions indicated a final radius R and a C_p value coherent with expected values for a 2.0 MW wind turbine blade. The same results may be compared with wind turbine blades commercially adopted.

This paper also presented a detailed formulation of the Vortex Lattice Method (VLM) for both flapped and twisted wing planforms. The proposed formulation has been implemented into MATLAB software and an user interface with pre-processor, solver and post-processor capabilities was developed to help designers to design morphing wing structures. A detailed description of the numerical implementation was also presented and discussed. Some modifications were implemented on the original MATLAB software for the use of wing turbine blades, especially related with the geometry of the blade and the $r\Omega$ dependency of the flow and inflow characteristics of the wind turbines. Numerical simulations were carried out for the same example studied before of a 2.0 MW wind turbine (Donadon, 2008).

This is the first steps of a roll work that is in development. The final objective is to have a computational package able to perform an optimal design for wind turbine blades, aerodynamic and structurally saying. This optimization will include geometrical and structural parameters and also will evaluate aerodynamic and structural performances.

Perhaps the great amount of necessary simplification introduced in these first steps of the work, the results obtained until here are coherent and promising. The pressure distribution has the form expected as also the total lift coefficient. Other results found at literature could confirm this. Some of thess results can be seen at figure 16 (Belessis, 1998).

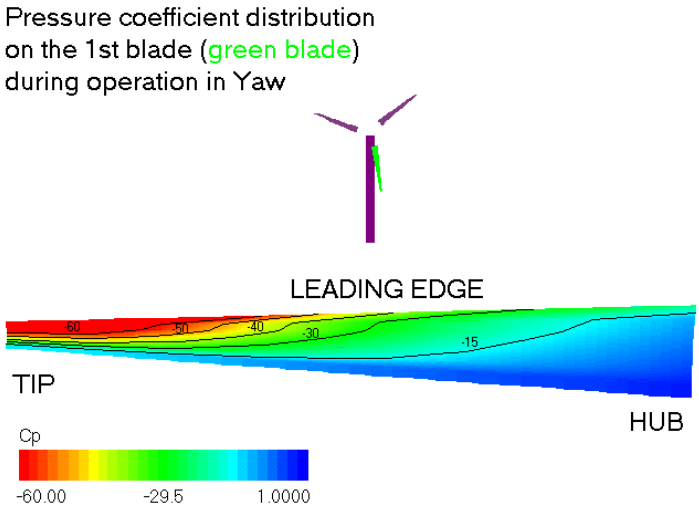

Figure 16. Pressure coefficient distribution graph.

Other classical results of lift and pressure distribution found were that related with the aerodynamics of helicopters. These distributions are classical and also compatible with the results found until now. Classical graphics of these distributions can be observed at figure 17.

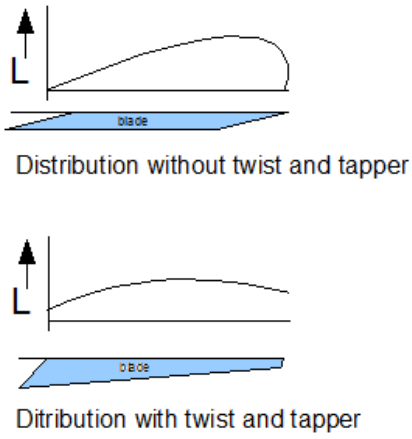

Figure 17. Pressure distribution on helicopters blades.

7 FUTURE WORK

The next steps of the work are the implementation of the procedure without the simplifications proposed until here. The use of optimal design of the blade, including the optimal chord distribution and the distribution of the twist angle is necessary.

Other important feature to be implemented is the camber of the foil used on the blade. The VLM can perform the calculation of the lift and pressure distribution using the camber line of the foil to generate the mesh. Best results related with the aerodynamic characteristics are

expected using this procedure.

The total torque of the turbine needs also to be compared with that one obtained by the BEM theory. And principally the variation of the power coefficient with the tip speed ratio will be compared with this same distribution given by BEM theory.

This both comparisons will validate the model and make possible future steps on this work.

8 ACKNOWLEDGEMENTS

The authors acknowledge the financial support received for this work from the Coordination of Improvement of Higher Education (CAPES) by the Institutional Program Teacher Qualification for the Federal Network of Professional Education, Science and Technology (PIQDTec) program of the Federal Technological University of Paraná (UTFPR).

The authors acknowledge the financial support received for this work from the Brazilian Research National Council (CNPq), contract number 303287/2009-8.

9 RESPONSIBILITY NOTICE

The authors are the only responsible for the printed material included in this paper.

REFERENCES

Belessis, M. A., 1998, National Technical University of Athens [on line]. Disposable on the internet via http://www.fluid.mech.ntua.gr/selavi/selavi.htm.

Bertin J. J., 1989 , Aerodynamics for Engineers, Prentice-Hall Inc., 2nd ed.

Burton,T., 2001, "Wind Energy Handbook", Ed. John Wiley and Sons Ltd., Chichester, New York, 624 p.

Do Nascimento, J. B., 1998, "Estudo Aerodinâmico do Efeito da Rugosidade no Desempenho de um Modelo de Turbina Eólica de Eixo Horizontal", Tese de Doutorado, USP – São Carlos, Brazil, 131 p.

Donadon, M. V.and Iannucci Lorenzo, 2006. "A Vortex Lattice Program to Compute Aerodynamic Loads in Flapped and Twisted Wings Planforms", Internal Report-Flaviir Seed Corn Project, Department of Aeronautics, Imperial College London.

Donadon, M. V., Savanov, R., Menezes and J. C., Moreira Filho, L. A., "A Numerical Tool to Design Blades for horizontal Axis Wind Turbines with Variable Geometry" V National Congress of Mechanical Engineering, CONEM 2008, Salvador, Bahia, Brazil.

Gash, R. and Twele, J., 2002, "Wind Power Plants", Ed. James & James (Science Publishers) Ltd., London, UK, 390 p.

Hansen, M.O.L., 2001, "Aerodynamics of Wind Turbines: Rotors, Loads and Structure", Ed. James & James (Science Publishers) Ltd., London, UK, 152 p.

Loftin, L.K. and Bursnall, W.J., 1948, "Effects of Variations in Reynolds Number between 3.0×10^6 and 25.0×10^6 Upon the Aerodynamic Characteristics of a Number of NACA Airfoil Sections, NACA TN-1773, NASA Langley

Menezes, J.C.and Donadon, M.V., 2009, "Optimum Blade Design of a 2 MW Horizontal Axis Wind Turbine", 20th International Congress of Mechanical Engineering, Gramado, RS, Brazil.